Optica Applicata, Vol. XXX, No. 1, 2000

Dynamics of molecular liquids studied by femtosecond optical Kerr effect

PIOTR WIEWIÓR, CZESŁAW RADZEWICZ

University of Warsaw, Institute of Experimental Physics, ul. Hoża 69, 00–681 Warszawa, Poland.

Femtosecond, time-resolved, optical-heterodyne detected optical Kerr effect (OHD-OKE) measurements are shown to be a powerful and comprehensive tool for studying the dynamics in molecular liquids. In our experiments the transient polarizability anisotropy of chloroform, carbon tetrachloride, carbon disulfide, benzene, benzonitrile and toluene has been measured with 30 fs laser pulses generated by a home-built Ti:Sapphire laser system.

1. Introduction

Our ability to study ultrafast processes in physics, chemistry and biology has been greatly boosted by the availability of a growing range of ultrashort-pulse laser sources and currently a wide range of processes that occur on nano-, pico- and femtosecond time scales can be investigated [1]. Given the importance of such processes, it is not surprising that a drive to better understanding of the ultrafast dynamics has, in turn, motivated the development of suitable laser sources for probing these transient events.

The ultimate time resolution in time-domain spectroscopic experiments can never be better than the inverse of the bandwidth of the excitation light used, as given by the fundamental restriction of the Fourier transformation. A light source providing the experimentalist with a potentially short optical pulse, must therefore inherently accommodate a large spread in photon frequencies.

The ability of the Ti:Sapphire solid-state oscillator to generate pulses of a few femtosecond duration [2] as well as its excellent reliability, make this laser an attractive ultrafast light source in the laboratory. Not surprisingly, the class of lasers based on Ti:Sapphire has rapidly gained ground in the field of ultrafast spectroscopy.

2. Theoretical background

Molecular dynamics of liquids can be investigated with a variety of experimental techniques such as: optical Kerr effect spectroscopy [3], time-resolved Stokes shift measurements [4], dielectric spectroscopy [5], X-ray diffraction [6] and neutron scattering [7]. The advent of nonlinear optical techniques and, especially, time resolved techniques due to impressive improvements of ultrafast laser technology

in the last decade opened up new possibilities of investigation in this field. One of the main advantages of time resolved experiments is the fact that they enable one to access, in a single measurement, a wide time range, thus providing an insight into different processes with widely different characteristic time scales. In particular, femtosecond optical Kerr effect (OKE) has emerged as a powerful technique in studying molecular dynamics in liquids.

In the OKE experiment, an intense femtosecond laser pulse (pump pulse) interacts with a liquid sample inducing a macroscopic polarization arising from nonlinear coupling between the electric field of the pump pulse and the sample. The signal is detected as a birefringence transient measured with a suitably delayed weak probe pulse. The experiment is usually performed with the laser detuned from any electronic resonances and no population is transferred between electronic states. In this case, because the Born–Oppenheimer approximation applies, the nonlinear optical response can be separated into electronic and nuclear components. These components include an effectively instantaneous response due to the electronic hyperpolarizability and a slower response due to the motion of nuclei in molecules. While femtosecond laser pulses are short, they certainly are not instantaneous, especially when electronic response is considered. Thus, the birefringence transient that we observe is a convolution of the molecular nonlinear response and the instrumental function which is determined primarily by the laser pulse duration.

The phenomena underlying the optical Kerr effect in liquids and molecular motions associated with them are summarized in Fig. 1. The electronic response is due to the nonlinear electronic polarizability (hyperpolarizability) of molecules. It is instantaneous on a time scale considered here and therefore its dynamics cannot be measured. All we can measure is the amplitude of the signal connected with electronic hyperpolarizability. Since the Born–Oppenheimer approximation holds and the interaction is non-resonant, the electronic hyperpolarizability is not accompanied by any motion of nuclei. The mechanisms of the non-instantaneous nuclear response associated with reorientational and interaction-induced dynamics can be classified as shown in Fig. 1. The term "reorientational dynamics" refers to rotational and translational motions of molecules and can be divided into nondiffusive and diffusive motions. The overdamped diffusive reorientational dynamics determine the long-time decay of the birefringence signal. The main mechanism of the susceptibility (birefringence) change is, in this case, the anisotropy of the molecular polarizability. While in a sample that is in equilibrium the molecules are randomly oriented, the interaction with a strong linearly polarized laser pulse tends to align them along one direction. This combined with the anisotropy of the molecular polarizability leads to a time-dependent birefringence of the sample. Although the diffusive reorientational motion decays exponentially for long delays, at short time delays the reorientational response should rise continuously from the equilibrium value (zero) up to a maximum. In the long-time range the motion is commonly described on the basis of the Debye–Stokes–Einstein hydrodynamic theory. This theory, which was developed to describe the rotational diffusion of a shpere in a featureless continuum, relates the rotational diffusion time τ_{rot} to the

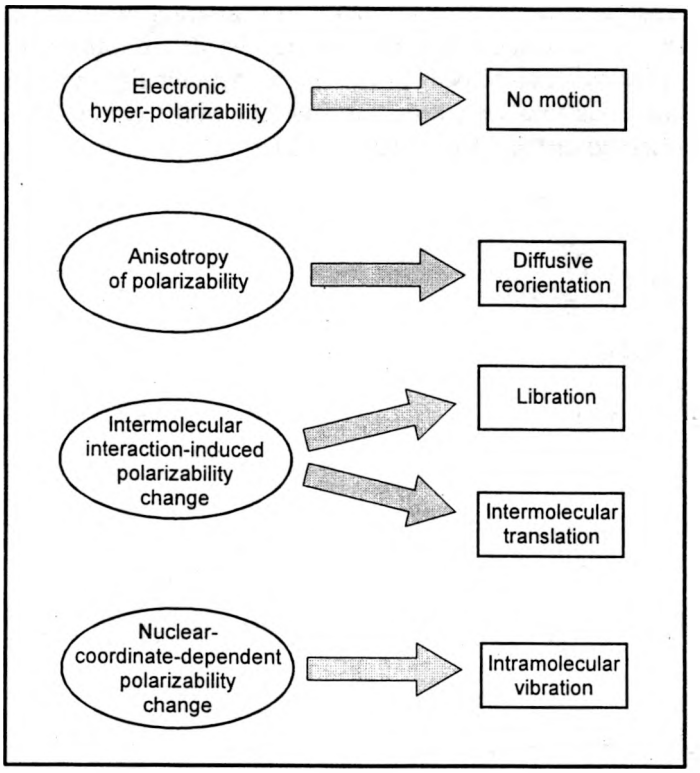

Fig. 1. Origins of the optical Kerr effect in liquids and the associated molecular motions.

bulk viscosity of the medium η, and the temperature T [8]

$$\tau_{\text{rot}} \propto V_{\text{eff}} \eta / kT. \tag{1}$$

The proportionality constant V_{eff} is the effective volume of the molecule associated with the rotation under examination. It depends on the size and shape of the molecule, as well as on the hydrodynamic boundary conditions.

The non-diffusive reorientational dynamics are all dynamics that are *not* strongly overdamped. These include rotations, librations and intermolecular translations. All of these motions contribute to the short-time response (typically <1 ps) of the birefringence signal. Librational motion is a small-angle oscillation of the orientation of molecules and can be regarded as a precursor of the diffusive reorientational motion in the OKE response. Librational motion affects the polarizability of the molecular system via the molecular polarizability anisotropy and the interaction-induced effect. Intermolecular translational motion affects the susceptibility only via the interaction-induced effect. An important and relatively poorly understood term responsible for the OKE response is the change of the polarizability due to the interaction between induced dipoles [9], [10]. In dense media, intermolecular translational motion can give rise to oscillatory features similar to those caused by the librational motion.

In addition to transients arising from reorientational and interaction-induced dynamics, an oscillatory feature corresponding to the impulsive excitation of intramolecular vibrational modes can also appear in the signal. Specifically, Raman modes with fundamental frequencies that lie within the spectral width of the laser pulse can be excited and observed in the Kerr signal [11].

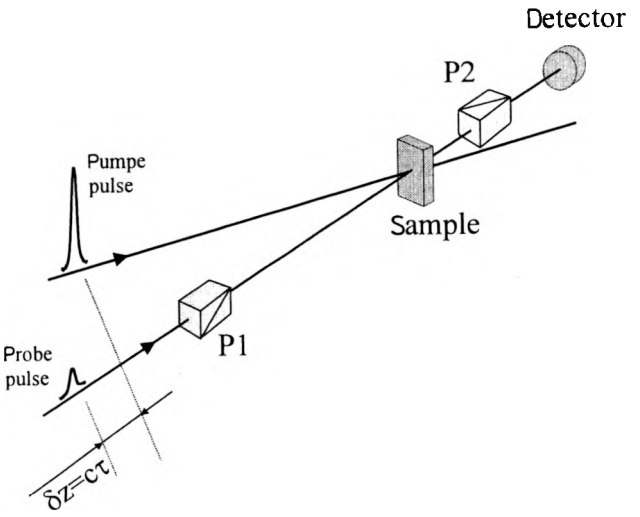

Fig. 2. Schematic diagram of the OKE experiment. P1 is a polarizer and P2 is an analyzer crossed with P1. The probe beam is polarized at 45° with respect to the pump beam.

The principles of the OHD-OKE method have been discussed in a number of recent papers, so we mention them only briefly here. In the optical Kerr effect, an intense linearly polarized laser beam generates nonlinear polarization in the medium which results in induced birefringence. A schematic diagram of OKE is shown in Fig. 2. For isotropic media such as liquids the susceptibility tensors of odd orders vanish due to the inversion symmetry. The lowest non-vanishing nonlinear polarization is then of the third order [12]

$$P_i^{(3)}(t) = \int_0^\infty \int_0^\infty \int_0^\infty dt_1 dt_2 dt_3 \chi_{ijkm}^{(3)}(t-t_1, t-t_2, t-t_3) E_j(t_1) E_k(t_2) E_m(t_3). \tag{2}$$

The relevant quantity in Eq. (2) is the third-order electric susceptibility of the medium $\chi_{ijkm}^{(3)}$. In experiments with femtosecond laser pulses the electromagnetic fields are applied in the form of ultrashort light pulses, and the different times that appear in Eq. (2) have a full physical meaning. In a typical experiment an intense linearly polarized pump pulse induces the birefringence at a given time. The probe pulse reaches the sample with a variable delay τ with respect to the pump pulse and probes the birefringence. The OKE signal $S(\tau)$ – the intensity of the probe pulse transmitted through the analyzer – at a given time delay τ is proportional to a double integral

$$S(\tau) \propto \int_{-\infty}^{\infty} I_{\text{probe}}(t-\tau)\left[\int_{-\infty}^{t} R(t-t')I_{\text{pump}}(t')\mathrm{d}t'\right]^2 \mathrm{d}t \tag{3}$$

where $R(t)$ is the response function of the system studied, and I_{probe} and I_{pump} are the intensities of the probe and pump beams, respectively. For isotropic media such as liquids the response function is given by

$$R(t) = \chi^{(3)}_{1111}(t) - \chi^{(3)}_{1122}(t). \tag{4}$$

A clear disadvantage of using OKE method as described above is that the signal measured in the experiment scales as a square of the molecular response function $R(t-t')$ which makes it difficult to interpret the experimental results. This can be easily avoided if one uses the OHD technique. The OHD-OKE method which is a pump-probe polarization spectroscopy scheme was first implemented in the frequency domain by EASLEY and LEVENSON [13] and then transferred into the femtosecond time domain by GREENE [14] and KENNEY-WALLACE and co-workers [15]. Optical heterodyning is achieved by providing a local oscillator field E_{LO}, in addition to the signal field, resulting in much higher sensitivity and signal-to-noise ratio. If the local oscillator field is coherent with the probe field, the total signal measured by the detector can be written in the form

$$I(t) \propto |E_{\text{LO}}(t) + E_{\text{S}}(t)|^2 \propto I_{\text{LO}}(t) + I_{\text{S}}(t) + 2\text{Re}\,[E^*_{\text{LO}}(t) \cdot E_{\text{S}}(t)] \tag{5}$$

where E_{S} is the signal field and I_{S} is the signal intensity. Because $|E_{\text{LO}}| \gg |E_{\text{S}}|$ (the experiment is set in such a way that the local oscillator field is much stronger than the signal field) the second term at the right hand side of Eq. (5) is small in comparison with the third term and can be neglected. Furthermore, by using lock-in detection one can eliminate the local oscillator intensity $I_{\text{LO}}(t)$ from the measured signal. As a result the signal measured in OHD-OKE experiment can be written in a linearized form

$$S(\tau) = \int_{-\infty}^{\infty} \mathrm{d}t E^*_{\text{LO}}(t-\tau) E_{\text{probe}}(t-\tau) \int_{0}^{\infty} \mathrm{d}t' R(t') |E_{\text{pump}}(t-t')|^2. \tag{6}$$

It is clear from Eq. (6) that the OHD-OKE scheme offers significant advantages. First of all, it increases the signal by a factor $|E_{\text{LO}}|/|E_{\text{S}}|$ which improves sensitivity and signal-to-noise ratio. In addition, the OHD-OKE method allows one to measure directly the material response function $R(t)$, instead of its square as is done in a standard OKE experiment.

3. Experimental setup

The experimental setup (the laser system and OKE apparatus) is shown in Figures 3 and 4.

3.1. Laser system

The laser system consists of a cw argon-ion laser (Coherent Innova 400) and a home-built, Kerr-lens mode-locked Ti:Sapphire laser with a Z-fold cavity con-

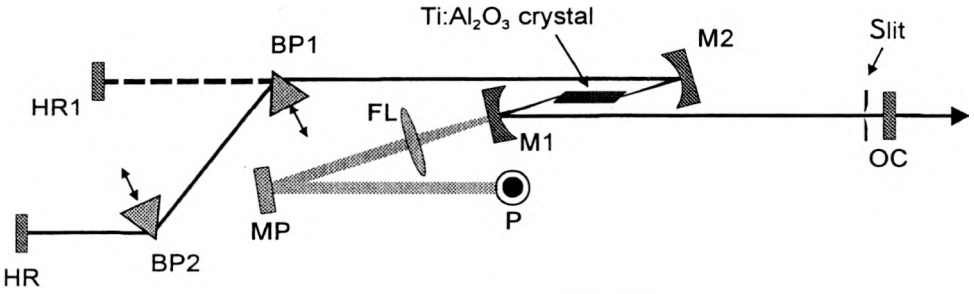

Fig. 3. Scheme of the femtosecond Ti:Sapphire laser used in the experiment: HR nad HR1 are flat high reflectors in the cavity with and without Brewster prisms, respectively, BP1 and BP2 are Brewster prisms, M1 and M2 are curved dichroic mirrors, OC is a flat output coupler. The pump beam from Coherent Innova 400 PowerTrack argon ion laser goes through a periscope P, and then it is reflected from a steering mirror MP and focused by a lens FL inside the $Ti:Al_2O_3$ crystal.

figuration shown in Fig. 3. The Ti:Sapphire laser resonator includes two curved dichroic mirrors transparent for the pump light and highly reflective for the laser radiation. Two flat mirrors complete the cavity, one acting as a high reflector and one as an output coupler. The two arms extending from the folded section are of slightly different length. The longer arm includes the dispersion compensation prisms. Two different regimes of operation can be selected, depending on the position of the prism BP1. For mode-locked operation the prism BP1 is inserted into the beam, thereby deflecting it towards the prism BP2 and the high reflector HR. For alignment purposes, the prism BP1 is retracted from the beam and the other high reflector (HR1) is used.

A 10 mm long Brewster-cut Ti:Sapphire crystal with 0.1% titanium concentration is placed in the center of the folded section. The crystal is pumped collinearly to obtain the best overlap between the pump beam and the resonator mode. A lens (FL) is used to focus the pump beam in the Ti:Sapphire crystal. The polarization of the laser mode is parallel to the optical table and defined by the lossless propagation at the Brewster surfaces of the crystal and the prisms, as well as the direction of the pump laser polarization and the laser crystal orientation. To minimize thermal lensing in the Ti:Sapphire crystal the crystal is cooled by running tap water.

The negative group delay dispersion (GDD) line necessary to obtain femtosecond pulse generation is formed by two Brewster angle LaK21 glass prisms. The choice of LaK21 glass is dictated by the requirement that the prism pair compensates the positive GDD of a 10 mm long Ti:Sapphire crystal with a reasonable prism separation distance. This particular glass has been selected because, in comparison with other types of glasses, it exhibits a relatively low amount of third-order dispersion. Prism separation of approx. 40 cm is needed to compensate for the dispersion of the Ti:Sapphire crystal. When operated without the prisms (with high reflector HR1) the laser generates approximately 0.8 watt of cw-radiation at 800 nm with 6 watts of pump power which gives conversion efficiency of about 13%. Insertion of the prism pair in the long arm of the resonator introduces additional

losses and reduces the output power to approx. 0.3 watts. The repetition rate of the laser is 102 MHz. The laser allows for routine and very stable generation of 30-fs duration pulses. Because the output pulses are chirped the output beam of the Ti:Sapphire laser is directed into a double-pass prism dispersion line in a near retro-reflection geometry. This arrangement not only compensates for the chirp in the laser pulse but also makes it possible to precompensate for the group velocity dispersion of the subsequent optical components, including a wave plate, beam splitters, lenses, polarizers and a sample cell input window.

3.2. OKE setup

The OHD-OKE setup is shown schematically in Figure 4. The pump-probe setup was equipped with a precision hollow corner cube attached to a precision linear stage driven by a stepper motor. This delay line was used to provide well defined and controlled delay between the pump and probe pulses. Operationally, the weak probe pulse was derived from the Ti:Sapphire laser pulse train by the use of a reflection from a beam-splitter (BS); the remainder of the pulse served as the strong pump beam. The time delay between probe and pump pulses was set by a personal computer controlling the stepper motor. Both beams were focused to a common spot (w_0 parameter in a focus spot was approx. 48 μm) in the sample with a lens L1, crossed in the sample at an angle of about 2 degrees and were recollimated afterwards. Two crossed crystalline polarizers P1 and P2 were placed in the probe beam path in such a way that the probe beam polarization direction formed a 45 degrees angle with the polarization direction of the pump beam. The pump beam was blocked behind the sample cell while the probe beam was steered into a PIN silicon photodiode (PD). To reduce the scattered pump beam light, the photodiode was placed approx. 2 m away from the sample region of the apparatus. The output of the photodiode was processed by a digital lock-in amplifier (Stanford Research Systems, SR 830 DSP) referenced to a mechanical chopper placed in the pump beam. For each position of the delay line the signal was recorded and stored in a personal computer. The measurements of the optical Kerr effect are quite sensitive to the quality of the optical elements. The pair of polarizers used in the experiment had an extinction ratio of the order of 10^{-6}. In practice, when high quality plarizers are used, the extinction is limited by the residual static birefringence of the lenses and the sample cell. First, this residual birefringence was minimized by using thin lenses made of high-quality glass. In addition, lenses L1 and L2 were mounted in rotational stages and rotated in order to minimize the leakage through the P2 polarizer. A 10 mm-path glass cell was used to hold the liquids studied. It was mounted on an X-Y translation stage and positioned to minimize both the probe leakage through the P2 polarizer and scattered pump light reaching the detector. The signal in a traditional OKE system (with two crossed polarizers) is quadratic in the material response. To enhance the sensitivity and avoid the necessity of analyzing a quadratic signal a heterodyne detection scheme described above was used. A local oscillator field for optical heterodyne detection scheme was derived with a mica quarter-wave plate placed in the probe beam behind the polarizer P1. Initially, the quarter-wave

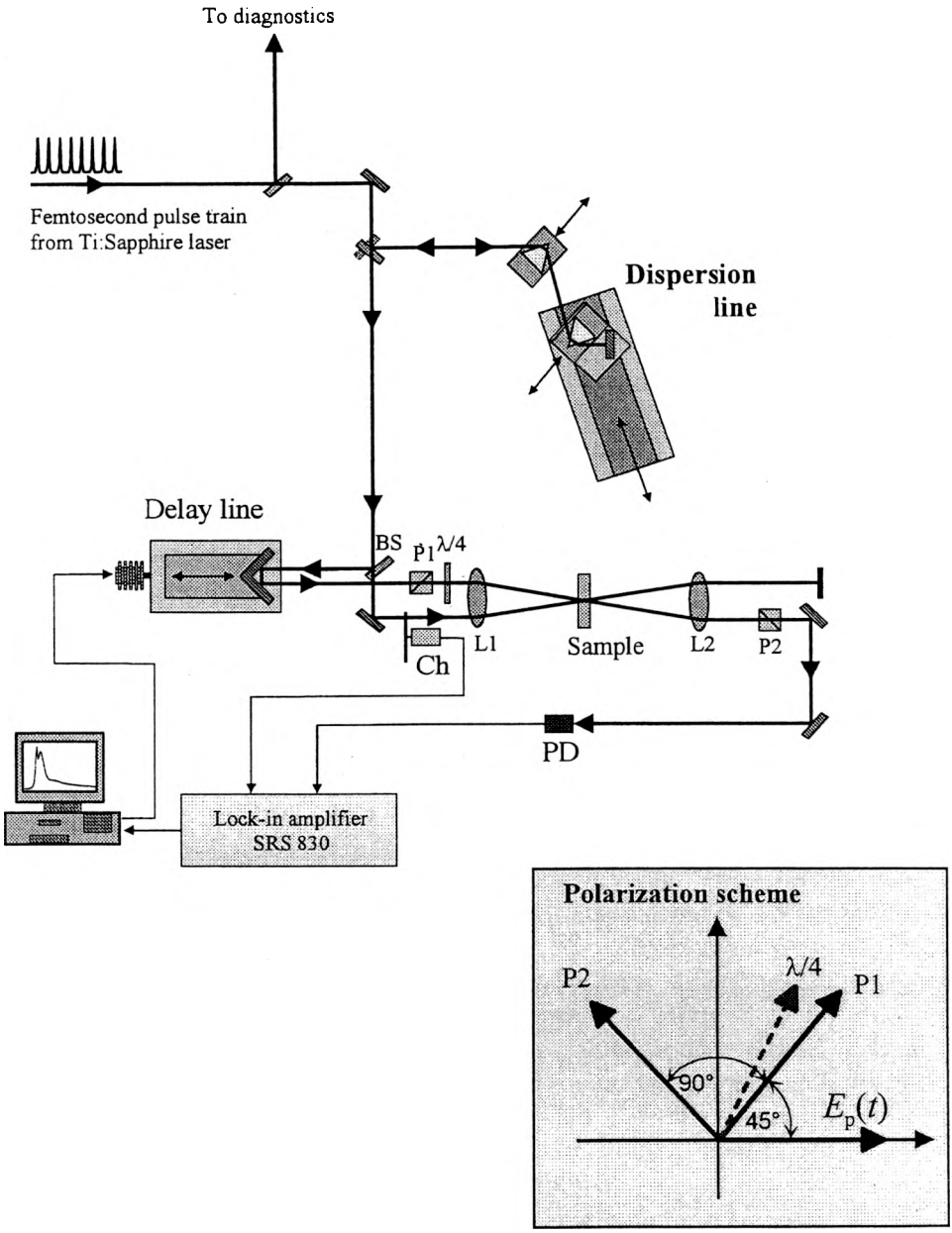

Fig. 4. An OHD-OKE apparatus. BS is a beam-splitter, P1 and P2 are a polarizer and an analyzer, respectively, $\lambda/4$ is a quarter-wave plate, L1 and L2 are the focusing and collimating lenses, respectively. Ch is a mechanical chopper that modulates the pump beam intensity and provides a reference frequency to the lock-in amplifier. The external dispersion line is shown as well as the polarization scheme.

plate was set so its fast axis was parallel to the probe beam polarization direction and the leakage through the system was minimized as described above. Then, to achieve homodyne detection (OHD-OKE scheme) the quarter-wave plate was rotated by approx. 1°. This yielded the local oscillator field of proper amplitude.

Samples with the spectroscopic grade of purity were purchased from manufacturers and used without further purification. The glass cell holding the liquids was temperature stabilized to ± 0.5 °C. We found that the Kerr signal was very noisy every time the cell was filled with fresh liquid. The noise level decreased over a time span of several hours and then stabilized. We attribute this noise to scattering of the pump light on dust particles suspended in the liquid. Given enough time the largest dust particles settle at the bottom of the cell and the signal quality improves considerably.

The time resolution in the OHD-OKE experiment is determined by two major factors: laser pulse duration (30 fs in our experiment) and dispersion of the optical components. We have used the external dispersion line to compensate for pulse broadening due to dispersion of all the optical components between the laser and the sample. The dispersion line has been optimized to minimize pulse duration at the interface between the input window of the sample cell and the liquid. This has been achieved by monitoring pulse duration with a home-built autocorrelator. However, a short pulse at the input face of the liquid sample does not necessarily mean high time resolution. One has to remember that the liquid itself is dispersive and broadens (in time) pump and probe pulses which decreases the time resolution of the experiment. Unfortunately, the external dispersion line cannot be used to compensate for this broadening – one can have the pulse short only in one given plane inside the sample. The only way to minimize this effect is to use a very thin sample. In our experiment the glass cell was rather thick (10 mm) which would imply a poor time resolution. This is not entirely true because the geometry of the experiment is such that the pump and probe beams cross (overlap) over a finite distance only. In our experimental setup that distance was approximately 3 mm. To take advantage of that fact, we translated the cell until the overlap region was located inside the liquid close to the input window of the cell. This procedure gave an effective sample thickness of 3 mm even though the actual length of the cell was 10 mm.

To measure femtosecond nondiffusive dynamics, short scans of a few hundred points over few picoseconds were taken with a time step of approx. 4 fs. To determine the diffusive dynamics, longer scans of a few thousand points over longer time delays were taken. Even with the most careful alignment there was always some amount of scattered pump beam measured by the detector. In order to account for this effect we have recorded the signal for negative delays (base line) and subtracted it from the data. The base line subtraction procedure is well justified as long as the laser power is constant during each scan.

4. Results and discussion

We present femtosecond OHD-OKE data obtained for six molecular liquids: carbon tetrachloride (CCl_4), chloroform ($CHCL_3$), carbon disulfide (CS_2), benzene (C_6H_6), benzonitrile (C_6H_5CN) and toluene ($C_6H_5CH_3$).

4.1. Carbon tetrachloride (CCl_4)

Femtosecond optical Kerr response measured for CCl_4 at room temperature is shown in Fig. 5. The curve is dominated by a single, strong and almost symmetrical peak at zero delay time. The CCl_4 molecule has an isotropic linear polarization and no relaxation processes connected with orientational motions of molecules are expected to contribute to the measured signal. Therefore it is reasonable to assume

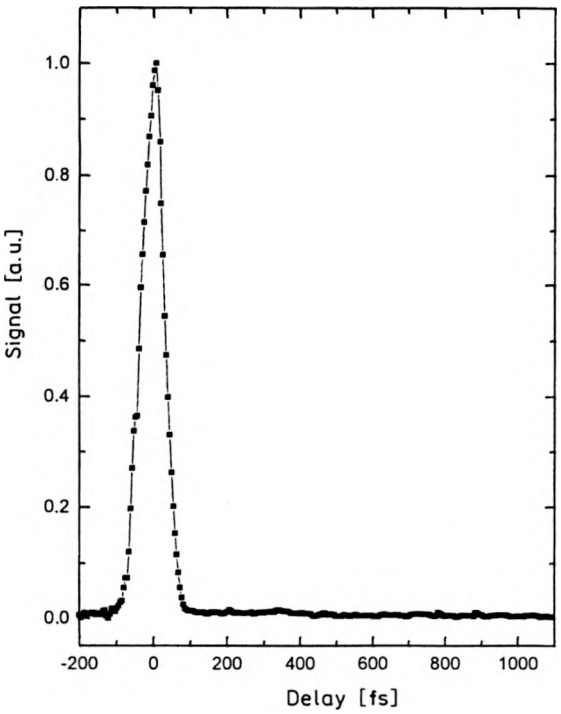

Fig. 5. Experimental OHD-OKE transient for carbon tetrachloride measured at room temperature.

that the peak observed in the experiment is entirely due to the electronic hyperpolarizability of the molecules which is instantaneous on the time scale considered here. In such a case the signal measured sould be proportional to the 2nd order intensity autocorrelation function of the laser pulse. Assuming that the laser pulse duration is 30 fs gives the FWHM of such autocorrelation function of approx. 50 fs. The FWHM of the measured curve is 65 fs. We conclude that the extra broadening observed in the experiment is due to the finite thickness of the sample.

4.2. Chloroform ($CHCl_3$)

According to the recent studies on CS_2 [16], nitrobenzene and chlorobenzene [16] and some chlorinated methanes [17] the full nonlinear response of the material can be separated into five components. Three of the five components can be categorized as non-resonant. These are: the orientational component attributed to a diffusive reorientational motion, the intermediate component attributed to density fluctuations in the bulk liquid, and the electronic component, which follows the excitation pulse. The other two components are resonant. The first is a low-frequency intermolecular libration. The second is an intramolecular vibration corresponding to low-frequency (<300 cm^{-1}) Raman modes of the molecules.

The Raman induced Kerr effect is well documented [18]. The restrictions on Raman modes observed with OKE are the same as for other motions to be detected by this method, *i.e.*, they must induce anisotropy in the sample. In Raman spectroscopy, the normal modes are categorized as "polarized" when the scattered light retains the polarization of the incident light, and "depolarized" when it does not. Anisotropic asymmetric modes are depolarized, and since the optical Kerr effect measures anisotropy, these modes can be detected by this method. By contrast, symmetric modes tend to be only weakly depolarized and are not expected to be easily detectable in the OKE experiment.

An ultrafast pulse is spectrally broad. The laser used in our experiments generates pulses of 30 fs duration and the spectral width of the pulse is sifficient to excite Raman modes with frequencies lower than 300 cm^{-1}. The $CHCl_3$ molecule investigated here has the C_{3v} symmetry and six Raman active modes. Three of these modes are totally symmetric (A_1 symmetry), while the other three are of the E symmetry. Recalling the restriction on Raman modes that can be detected with the OKE method and the finite spectral width of our laser one finds that only the E modes with frequencies below 300 cm^{-1} can be detected. It is important to note that all Raman active modes of the molecule with frequencies below 300 cm^{-1} are excited by the coherent Raman process. However, only the modes that introduce significant optical anisotropiy can be detected in our experiment.

Figure 6 shows the data obtained for $CHCl_3$ at room temperature. The Kerr signal is again dominated by the electronic component, however, the data show at least one oscillatory component in the decay curve. The oscillatory component, corresponding to the coherently excited Raman mode, was fitted with the following formula:

$$S(t) = S_0 \exp\left(\frac{-t}{\tau_{osc}}\right) \sin(\omega_{osc} t). \tag{7}$$

The frequency ω_{osc} can be easily obtained from a Fourier transform of the experimental data. Once ω_{osc} is determined the amplitude of the Raman signal S_0 and the lifetime of the oscillations τ_{osc} are found by fitting the data with formula (7). Such an analysis gives for our data the following values: the oscillation decay time $\tau_{osc} = 1.5$ ps and the frequency of Raman oscillations $\omega_{osc} = 262$ cm^{-1}. The decay of

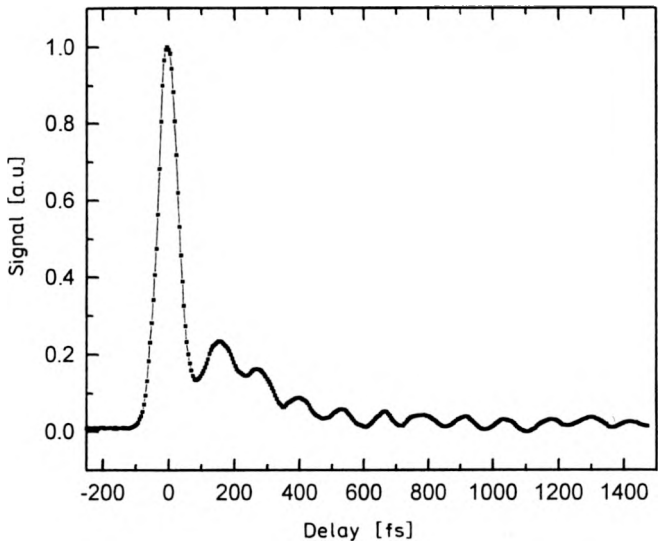

Fig. 6. Experimental OHD-OKE transient for chloroform measured at room temperature.

the oscillations apears to be homogeneous, manifested in a single exponential decay with a characteristic lifetime τ_{osc}. This would imply that all of the oscillators for a given mode are in phase at the time of excitation, but due to collisions, the signal from the oscillation decays with time. Two types of collisions occur: elastic collisions do not permit energy transfer between colliding species, but a loss of phase can lead to dephasing of the coherent Raman signal; in inelastic collisions energy can be transferred between colliding molecules, leading to a destructive interference between oscillators and to depopulation. Both of these processes lead to a homogeneous decay of the oscillatory component in the signal. The decay time of the oscillations is shorter than the diffusive reorientational time which was also determined from our data as $\tau_{orient} = 2$ ps. This indicates that the mechanism of decay is not limited to orientational collisions, but may have contributions from translational collisions as well.

The table lists the frequencies of the Raman modes for the $CHCl_3$ molecule taken from [19]. We observe only one Raman mode in the OKE experiment. According

T a b l e. Frequencies of Raman modes in $CHCl_3$ molecule.

Mode	Frequency [cm^{-1}]
ν_1	3179
ν_2	686
ν_3	–
ν_4	1262
ν_5	782
ν_6	264

to restrictions discussed earlier, we expect that the observed Raman mode is the lowest-frequency asymmetric mode ν_6 associated with an asymmetric deformation of the CCl_3 group. The frequency of the ν_6 mode is equal to 264 cm^{-1} and this value is very close to the value obtained from our experimental data $\omega_{osc} =$ 262 cm^{-1}.

4.3. Carbon disulfide (CS_2)

Figure 7 illustrates the complexity of the Kerr response for neat CS_2 at room temperature. The signal shows an initial feature centered at $t = 0$ which is due to the essentially instantaneous electronic response of the medium. This feature appears in all materials and persists only while the excitation and probe pulses overlap in time.

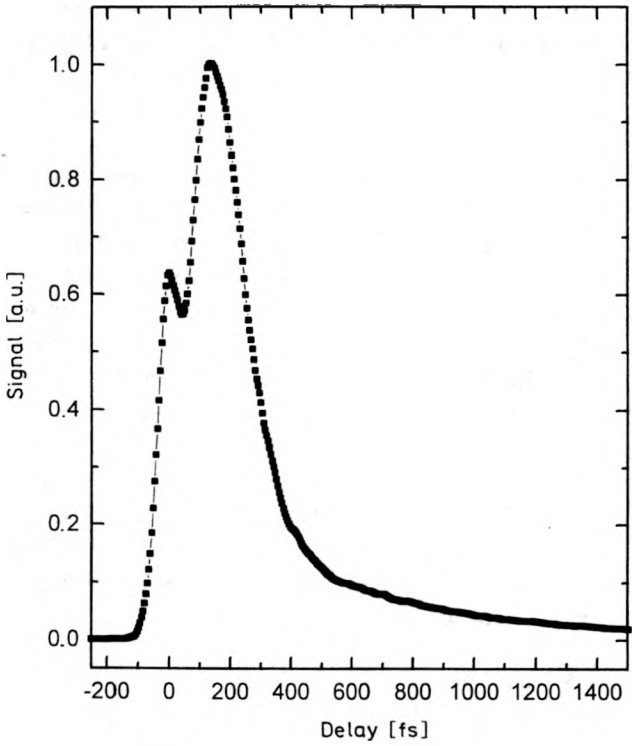

Fig. 7. Experimental OHD–OKE transient for carbon disulfide measured at room temperature.

After the electronic response has reached maximum at zero-delay time, there is a more gradual increase in the signal with another maximum at $t \approx 150$ fs. This rise occurs because of the inertial response of the CS_2 molecules to the nearly instantaneous excitation force. The molecular motions do not occur instantaneously, but rather continue away from the equilibrium after the excitation pulse has passed the sample. After reaching the maximum the signal decays rapidly and then more slowly. The rapid decay, we believe, is due to a reversal in directions of the initial

molecular motions. The reversal results primarily from intermolecular repulsion between "colliding" molecules. In other words, the short-time dynamics reflect intermolecular vibrational motion in the liquid [20].

A detailed data analysis demonstrates the presence of four distinguishable contributions to the Kerr signal in neat CS_2 (errors in all the amplitudes $A_1 - A_4$ are $\pm 5\%$, $A_1 + A_3 + A_3 + A_4 = 1$):

– A purely electronic, instantaneous hyperpolarizability contribution with relative amplitude $A_1 = 0.27$.

– A contribution due to a rapidly dephasing, coherently excited intermolecular librational motion (molecular "rocking") – relative amplitude $A_2 = 0.39$, decay time $t_2 = 140$ fs. This rapidly decaying oscillatory response is absent in liquids composed of isotropic species, and thus is associated with the orientational motion of anisotropic molecules. Accordingly, this response has been assigned to a coherently driven, Raman-active, intermolecular librational motion [16]. The decay time for this component τ_2 gives the characteristic time scale for fluctuations in the local liquid structure and provides information about the nature of the *local* intermolecular potential.

– An intermediate contribution with an exponential decay associated with intermolecular interactions – relative amplitude $A_3 = 0.14$, decay time $\tau_3 = 440$ (± 50) fs. The "interaction-induced" distortion of the molecular polarizability is a many-body effect, ascribed in CS_2 primarily to interaction between induced dipoles. Within the Born–Oppenheimer approximation, intermolecular interaction-induced contribution to the signal adiabatically follows the nuclear translational and orientational motions of the anisotropic molecular species.

– The slowest contribution associated with exponentially decaying orientational anisotropy – relative amplitude $A_4 = 0.20$, decay time $\tau_4 = 1.65$ (± 0.05) ps. Like the librational contribution, the orientational response is absent in liquids composed of isotropic molecular species. This response is assigned to the imposition and decay of an anisotropic distribution of molecular orientations [16]. The anisotropy is induced by the intense optical field, and subsequently decays through the random, thermal fluctuations of the liquid.

4.4. Benzene (C_6H_6), toluene ($C_6H_5CH_3$) and benzonitrile (C_6H_5CN)

Femtosecond OHD-OKE data for benzene, toluene and benzonitrile at room temperature are shown in Fig. 8 for a time range of about 4 ps. The insets show the same data for a time range of about 1.5 ps. For all these birefringence transients the initial short spike due to electronic hyperpolarizability is followed by an additional peak which decays multiexponentially.

In the case of benzene the long time component decays with a time constant of 2.5 (± 0.1) ps, which is in excellent agreement with previously published results [21]. This 2.5 ps decay time can be assigned to the diffusional reorientation time around the C_2 axis of the benzene molecule. The benzene molecule has two principal, independent rotational moments of inertia, and therefore, in principle, we should expect two rotational relaxation times. Besides the tumbling motion around

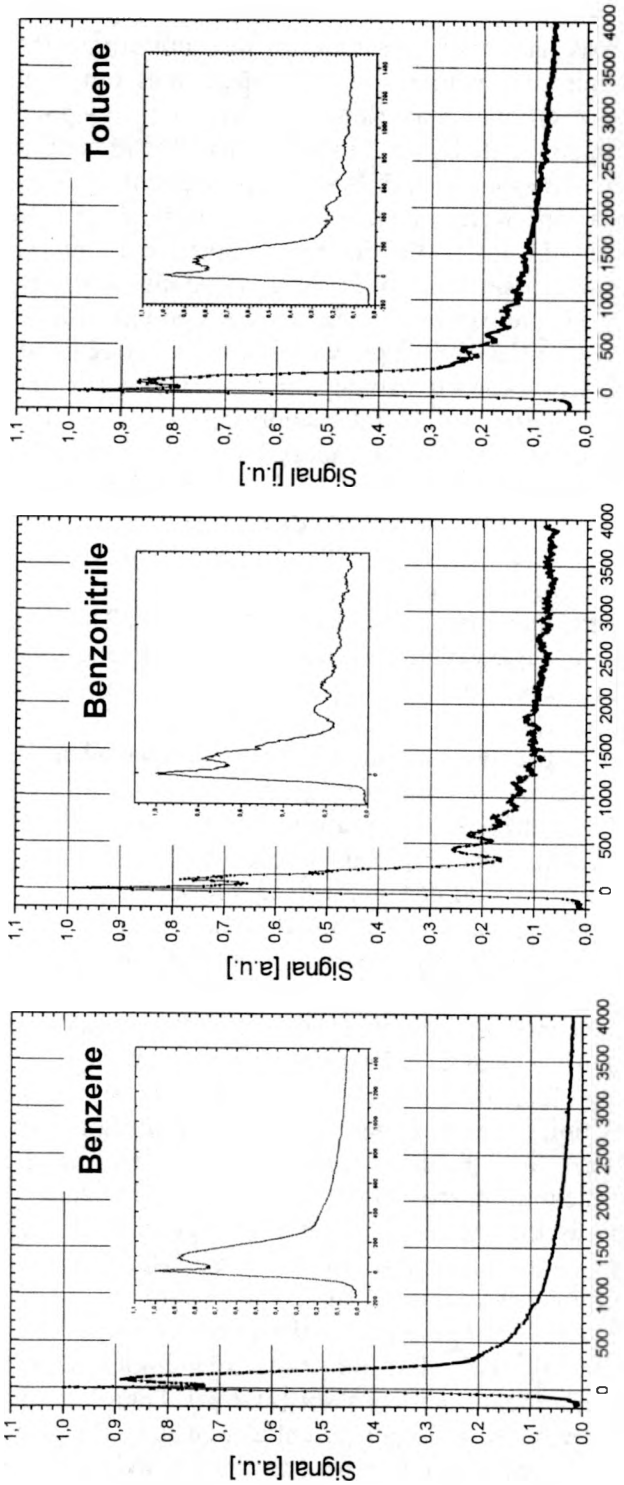

Fig. 8. Experimental OHD-OKE transients for benzene (left panel), benzonitrile (middle panel) and toluene (right panel) measured at room temperature. The insets show the signals for shorter delays.

the C_2 axis, there is another rotational degree of freedom corresponding to the spinning motion around the C_6 axis. However, this motion does not rotate the polarizability ellipsoid in a distinguishable manner, and therefore does not contribute to the Kerr signal. The 2.5 ps rotational relaxation time is also in a very good agreement with the results from the stimulated gain measurements [22] as well as with the analysis based on Raman line-shapes and NMR measurements [23].

The central panel in Fig. 8 shows the Kerr transient for benzonitrile from 0 to 4 ps; a 0–1.5 ps scan is plotted in the inset. The long time component of the time-dependent signal can be fitted with a single exponential, giving diffusional time constant of 21.2 ps. The 21.2 ps component can be assigned to the tumbling motion around the axis that is in the molecular plane and is perpendicular to the CN bond. The long decay time indicates that this rotation is strongly hindered due to a strong dipole–dipole interaction between CN groups. The interaction induces more local ordering in benzonitrile liquid and thus increases the energy barrier for tumbling, thereby slowing down the motion. It is reflected in the increased viscosity of benzonitrile (1.24 cP) as compared to that of benzene (0.61 cP). At delays longer than 300 fs an underdamped oscillatory feature corresponding to the intramolecular C–CN torsional mode at approx. 170 cm^{-1} is also visible.

The Kerr signal for toluene is shown in the right hand panel in Fig. 8. The long time component has been fitted with a single exponential decay giving the relaxation time constant of approx. 6 ps. The oscillations corresponding to intramolecular $C-CH_3$ torsional mode at approx. 220 cm^{-1} are also evident.

The intermolecular interactions in benzonitrile and benzene are expected to be significantly different. Because benzonitrile has a large dipole moment of 4.18 D, dipole–dipole interactions should contribute significantly to the overall intermolecular interaction in the liquid. This is clearly seen by comparing the boiling points for both liquids: 353 K for benzene and 464 K for benzonitrile. Benzonitrile has larger polarizability and larger polarizability anisotropy than benzene. The local structure of benzonitrile should be qualitatively different from that of benzene because of the less-symmetric molecular shape and the strong dipole–dipole interaction. But the experimental data show that the short-time-scale Kerr signals for benzene and benzonitrile are qualitatively similar. The reason for this similarity lies in the nature of the librational motions that contribute to the Kerr signal. In benzonitrile, the dominant contribution to the Kerr response comes from librations around two principal axes (the CN axis, and the axis within the molecular plane and perpendicular to the CN axis). For the motion around the CN axis, the polarizability change is approximately the same as that in benzene rotating around a C_2 axis – the moments of inertia for the two molecules are also the same. Thus, one can expect that the corresponding librational motions will be similar in both molecules. This does not necessarily apply to the motion around the other principal axis. Benzonitrile molecules must be at least partially aligned by the strong dipole–dipole interactions as indicated by the long orientational constant (21.2 ps). Therefore, the tumbling motion of CN axis will experience a deeper potential well than the same motion for benzene, even though the spinning motion around the CN axis will not

be significantly influenced. The libration that is perpendicular to the CN axis will experience a larger polarizability change and a deeper potential well relative to the benzene. However, the moment of inertia for this libration is much larger than for benzene. Because of these two compensating factors, the short-time-scale part of the Kerr signal from benzonitrile is not much different from that for benzene.

5. Summary and conclusions

Femtosecond OHD-OKE technique allows one to observe directly, in the time domain, short-time dynamics which are difficult to characterize in the frequency domain. We have described the experimental determination of the femtosecond dynamics of the off-resonant femtosecond optical Kerr effect in selected neat molecular liquids (carbon tetrachloride, chloroform, carbon disulfide, benzene, toluene and benzonitrile). The OHD-OKE transients for investigated liquids are dominated at early times by the electronic heperpolarizability. The non-instantaneous nuclear response at early times is well described by three components: librational, intermediate and diffusive. An oscillatory feature was found in the OHD-OKE transients of neat chloroform, toluene and benzonitrile. This feature was attributed to molecular vibrational modes, which change the optical susceptibility of the liquids either via the molecular polarizability anisotropy or via the interaction-induced polarizability change.

Acknowledgements — This research was supported by a State Committee for Scientific Research (KBN), Poland, Grant No. 2 P03B 001 14.

References

[1] MANZ J., WÖSTE L., [Eds.], *Femtosecond Chemistry*, VCH Verlagsgesellschaft, Weinheim, New York 1995.
[2] XIU L., SPIELMANN CH., KRAUSZ F., SZIPOCS R., Opt. Lett. **21** (1996), 1259.
[3] MCMORROW D., Opt. Commun. **86** (1991), 236.
[4] JIMENEZ R., FLEMING G.R., KUMAR P.V., MARONCELLI M., Nature **369** (1994), 471.
[5] PEDERSEN J., IEEE J. Quantum Electron. **28** (1992), 2302.
[6] SETTE F., KRISCH M.H., MASCIOVECCHIO C., RUOCCO G., MANACO G., Science **280** (1998), 1550.
[7] BODENSTEINER T., MORKEL C., GLASER W., DORNER B., Phys. Rev. A **45** (1992), 5709.
[8] KIVELSON D., [In] *Rotational Dynamics of Small and Macromolecules*, [Eds.] T. Dorfmuller, R. Pecora, Springer-Verlag, Berlin 1987.
[9] VAN DER ELSKEN J., HULTS R.A., J. Chem. Phys. **88** (1988), 3007.
[10] GEIGER L.C., LADANYI B. M., Chem. Phys. Lett. **159** (1989), 413.
[11] YAN Y.-X., NELSON K.A., J. Chem. Phys. **87** (1987), 6240.
[12] MAKER P.D., TERHUNE R.W., Phys. Rev. **137** (1965), A801.
[13] LEVENSON M.D., EASLEY G.L., Appl. Phys. **19** (1979), 1.
[14] GREENE B.I., FARROW R.C., Chem. Phys. Lett. **98** (1983), 273; GREENE B.I., FLEURY P.A., CARTER H.L., FARROW R.C., Phys. Rev. A **92** (1984), 271.
[15] KALPOUZOS C., LOTSHAW W.T., MCMORROW D., KENNEY-WALLACE G.A., J. Phys. Chem. **91** (1987), 2082.
[16] MCMORROW D., LOTSHAW W.T., KENNEY-WALLACE G.A., IEEE J. Quantum Electron. **24** (1988), 443; RUHMAN S., WILLIAMS L.R., JOLY A.G., KOHLER B., NELSON K.A., J. Phys. Chem. **91** (1987), 2237.

[17] MCMORROW D., LOTSHAW W.T., KENNEY-WALLACE G.A., Chem. Phys. Lett. **145** (1988), 309; RUHMAN S., JOLY A.G., NELSON K.A., J. Phys. Chem. **86** (1987), 6563.
[18] EESLEY G.L., *Coherent Raman Spectroscopy*, Pergamon Press, Oxford 1981; LEVENSON M.D., *Introduction to Nonlinear Laser Spectroscopy*, Academic Press, New York 1982.
[19] BERMEJO D., ESCRIBANO R., ORZA J.M., Raman Spectrosc. **6** (1977), 151.
[20] RUHMAN S., WILLIAMS L.R., JOLY A.G., KOHLER B., NELSON K.A., J. Phys. Chem. **91** (1987), 2237.
[21] MCMORROW D., LOTSHAW W.T., Chem. Phys. Lett. **201** (1993), 369.
[22] FRIEDMAN J.S., LEE M.C., SHE C.Y., Chem. Phys. Lett. **186** (1991), 161.
[23] GILLEN K.T., GRIFFITHS J.E., Chem. Phys. Lett. **17** (1972), 359.

Received November 16, 1999
in revised form March 20, 2000